Biochimica et Biophysica Acta 1808 (2011) 597–605

Contents lists available at ScienceDirect

Biochimica et Biophysica Acta

journal homepage: www.elsevier.com/locate/bbamem

Ouabain-induced modifications of prostate cancer cell lipidome investigated with mass spectrometry and FTIR spectroscopy

Régis Gasper, Guy Vandenbussche, Erik Goormaghtigh *

Laboratory for the Structure and Function of Biological Membranes, Center for Structural Biology and Bioinformatics, Université Libre de Bruxelles (ULB), Brussels, Belgium

ARTICLE INFO

Article history:
Received 5 October 2010
Received in revised form 25 November 2010
Accepted 30 November 2010
Available online 7 December 2010

Keywords:
IR spectroscopy
Mass spectrometry
Ouabain
Cancer
Drug
Lipid
Hetero-spectral correlation

ABSTRACT

Fourier transform infrared (FTIR) spectroscopy was used to investigate modifications of prostate cancer PC-3 cell lipidome after exposure to sub-lethal concentrations of ouabain. FTIR spectroscopy offered an overview of the lipid classes present in the whole sample. The method is simple, label free and some features can be detected on entire cells. We compared the achievements of FTIR spectroscopy with data obtained by mass spectrometry (MS) on the same samples. It appears that FTIR spectroscopy could identify content variations in some lipid classes, e.g., these containing choline head groups such as phosphatidylcholine and sphingomyelin. MS analysis could confirm this result as indicated by principal component analysis and 2D heterocorrelation maps. FTIR spectra were also able to report changes in ester/choline/phosphate ratios characterizing lipid changes induced by ouabain. Furthermore, quantization of major lipid classes (PC, PE, PG, SM) could be obtained by curve fitting of the FTIR spectra. Yet, FTIR failed to resolve lipid classes for which the polar heads do not display specific IR features such as phosphatidylglycerol and cardiolipin.

1. Introduction

Lipids are known to be involved in many biological pathways and modification of cell lipid composition can lead to severe pathologies [1,2]. For example, sphingolipids turned out to be key players in various cellular processes [3–6] and it was reported that sphingolipid disregulation can lead to tumorigenesis [7]. In turn, lipidomics is becoming an expanding field of research, which could contribute to the discovery of new biomarkers for several disease. For this purpose, mass spectrometry is a tool of choice [8,9], as the improvement of this technique for lipid analysis combined with sophisticated computational methods has facilitated the characterization of hundreds of phospholipid species from mammalian cell extracts [10,11].

Fourier Transform infrared spectroscopy became a powerful tool in the analysis of biological sample [12]. Development of modern Fourier Transform spectrophotometer coupled with statistical analysis of FTIR spectra provides accurate fingerprints of samples under study [13]. In turn, bacteria or yeast typing at strain level can be performed [14,15] as well as differentiation between cell lines in culture or in tissue slices [16–18]. Recently, FTIR spectroscopy was used with success for identification of PC-3 lipid content modifications induced by sub-lethal concentration of ouabain [19]. Ouabain is one of the most studied cardenolide, a promising family of compounds with anti-tumoral activities (for a detailed review see, [20,21]).

While, mass spectrometry is highly efficient for discrimination and identification of single molecule species, it requires complex experiments to be quantitative. FTIR spectroscopy easily provides an accurate global fingerprint of every chemical bond present in the sample under study, qualitatively as well as quantitatively, but displays poor resolution when precise molecular structures are to be identified. The purpose of this paper is to investigate the combination of both techniques to analyse lipid extracts from cells grown in the absence or in the presence of sub-lethal concentrations of ouabain for different incubation times.

2. Materials and methods

2.1. Compounds

Ouabain was purchased from Acros Organics (Geel, Belgium). Dipalmitoylphosphatidylcholine (DPPC), dipalmitoylphosphatidylethanolamine (DPPE), dipalmitoylphosphatidylglycerol (DPPG) and sphingomyelin (SM) were purchased from Avanti Polar Lipids, Inc. (Alabaster, Alabama).

Abbreviations: FTIR, Fourier transform infrared; MS, mass spectrometry; PCA, principal component analysis; PC, phosphatidylcholine; PE, phosphatidylethanolamine; PG, phosphatidylglycerol; PS, phosphatidylserine; SM, sphingomyelin; PI3K, phosphatidylinositol-3 kinase

* Corresponding author. Center for Structural Biology and Bioinformatics, Laboratory for the Structure and Function of Biological Membranes, Campus Plaine CP206/02, Université Libre de Bruxelles, Bld du Triomphe 2, CP206/2, B1050 Brussels, Belgium. Tel.: +32 2 650 53 86; fax: +32 2 650 53 82.
E-mail address: egoor@ulb.ac.be (E. Goormaghtigh).

0005-2736/$ – see front matter © 2010 Elsevier B.V. All rights reserved.
doi:10.1016/j.bbamem.2010.11.033

2.2. Cell culture

The human prostate cancer PC-3 (CRL-1435) cell line was obtained from the American Type Culture Collection (ATCC, Manassas, VA) and was maintained according to the supplier's instructions. The cells were incubated at 37 °C in sealed (airtight) Falcon plastic dishes (Nunc, Invitrogen SA, Merelbeke, Belgium) in a humidified atmosphere of 5% CO_2. The cells were kept in exponential growth in RPMI

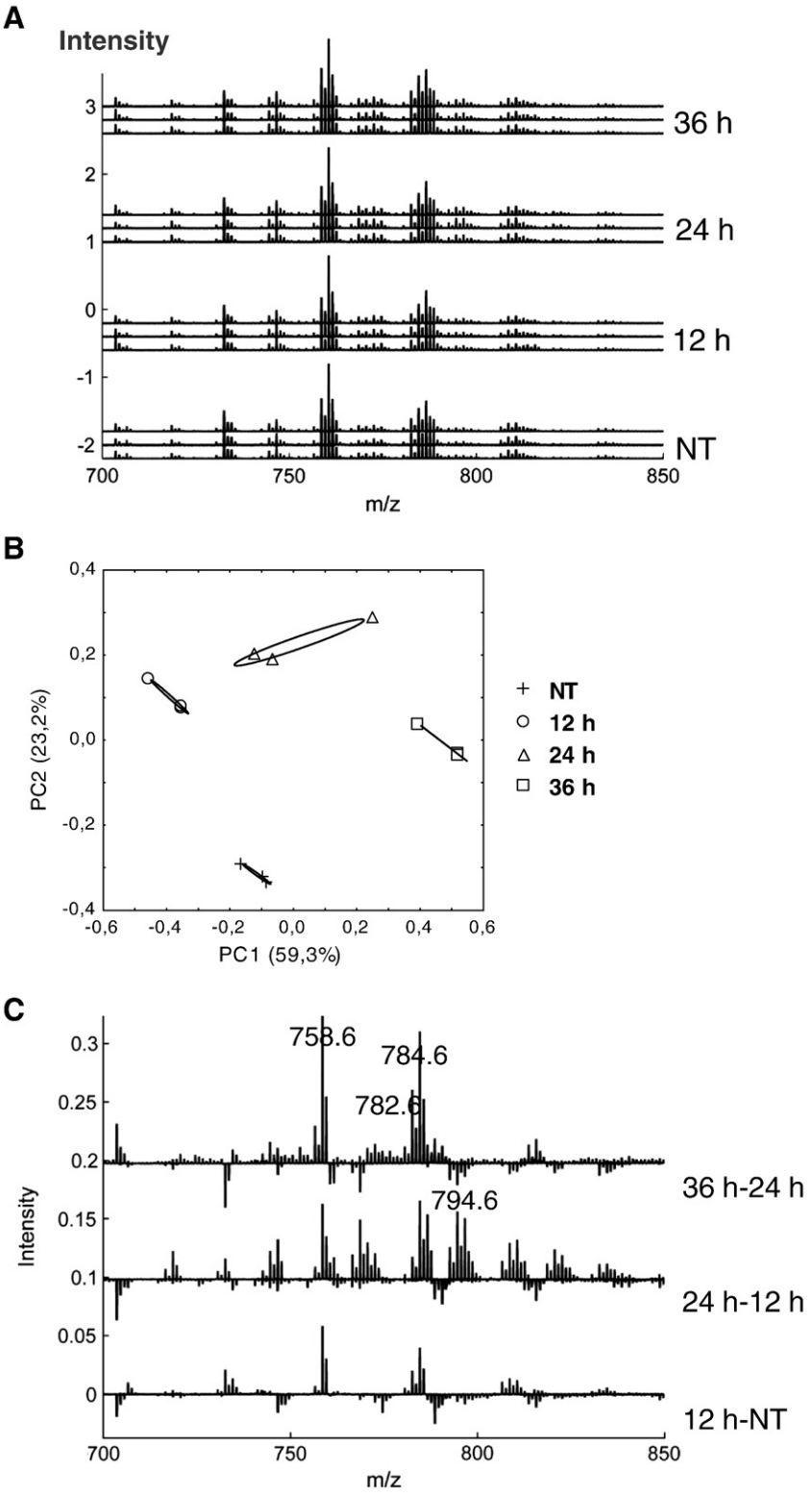

Fig. 1. (A) Mass spectra (positive ion mode) of lipid extracts from PC-3 cells incubated in the presence of ouabain for different periods of time. Every spectrum has been rescaled to the same intensity of the major peak, i.e., m/z 760.5869. Each mass spectrum originates from an independent cell culture. NT, 12, 24 and 36 are respectively lipids from cells exposed for 0, 12, 24 and 36 h to the drug. Spectra have been offset for better readability. (B) PCA performed on the mass spectra presented in A. Each symbol is the projection of one original mass spectra projected in the space of the two first principal components. *, ○, Δ, □ are lipids from cells exposed respectively to 0, 12, 24 and 36 h to 36 nM ouabain. Numbers between brackets represent the percentage of variance hold in each principal component. 95% confidence interval ellipses are presented. (C) Difference between pairs of mean mass spectra from successive conditions.

medium supplemented with 10% fetal bovine serum (FBS), 1% penicillin/streptomycin (an antibiotic/antimycotic solution), and 1% kanamycin to prevent mycoplasms. Medium and FBS were purchased from Gibco (Invitrogen, Merelbeke, Belgium). Penicillin/strepromycin and kanamycin solutions came from Sigma-Aldrich SA (Bornem, Belgium).

PC-3 cells were incubated with ouabain during 12, 24 and 36 h at its IC_{50}. The IC_{50} is defined as the concentration needed for decreasing the global cell growth of the cancer cells by 50% after 72 h of culturing, as assessed by MTT assay. IC_{50} of ouabain for PC-3 cell line is 36 nM [19].

Cells were suspended by means of a 5-min treatment with 3 ml trypsin (0.5 g/L)/EDTA (0.2 g/L) buffer (Gibco, Invitrogen SA, Merelbeke, Belgium) for 75 cm^2 culture plate. The reaction was stopped by adding 1 ml of culture medium. The cells were pelleted by a 2-min centrifugation ($300\times g$), and washed three times in isotonic solution (NaCl, 0.9%) to ensure complete removal of trypsin and culture medium. Cells were then quickly washed in pure desalted water and pelleted by a 2-min centrifugation ($300\times g$) to remove salts which could reduce the quality of mass spectroscopy experiments. Three independent cultures were grown for each ouabain condition. Microscopic observation (40×) revealed PC-3 cells to be intact.

2.3. Lipid extraction

Total lipid extract from PC-3 cells was obtained according to the protocol of Bligh and Dyer [22]. Briefly, three steps were carried out: (i) addition of 125 µl of chloroform/250 µl of methanol to 100 µl of sample and vortexing of the resulting solution, (ii) addition of 8.4 µl of hydrochloric acid (6 M) and 125 µl of chloroform and vortexing of the solution, (iii) addition of 125 µl of pure desalted water, vortexing of solution again, and centrifugation for 10 min at $300\times g$. Total lipid extract was collected in the lower phase.

2.4. Mass spectrometry

The mass spectra were acquired on a Q-Tof Ultima mass spectrometer (Waters, Micromass, Milford, USA), equipped with a Z-spray nanoelectrospray source and operating in the positive and negative ion modes. The total lipid extract was loaded into gold-palladium-coated borosilicate nanoelectrospray capillaries (Proxeon, Odense, Denmark). Capillary voltages of 1.1–1.5 kV and a cone voltage of 50 V were typically used. The source temperature was held at 80 °C. Data acquisition was performed using a MassLynx 4.0 system. The spectra represent the combination of 1-s scans. For the collision-induced dissociation (CID) measurements, the precursor ions were selected in the quadrupole and collided with argon in the hexapole collision cell using appropriate collision energy (typically 20–40 eV). For each condition (i.e., incubation time), three independent cultures were grown and one mass spectrum was recorded in positive as well as in negative ion mode for each culture. Positive ion mass spectra were recorded between m/z 500 and 900, while negative ion mass spectra were recorded between m/z 500 and 1500, both with a sampling of 0.0001 m/z.

2.5. FTIR spectroscopy

All measurements were carried out on a Bruker Equinox 55 FTIR spectrometer (Bruker, Karlsruhe, Germany) equipped with a liquid N_2-refrigerated mercury cadmium Telluride detector. All spectra were recorded by attenuated total reflection (for a review, see [23]). A diamond internal reflection element was used on a Golden Gate Micro-ATR from Specac (Orpington, UK). The angle of incidence was 45°. Lipid extracts used for FTIR analyses are the same as those used for MS spectrometry experiments. The sample was evaporated under a gaseous N_2 flow to form a thin film. In these conditions, solvent removal is completed in less than a minute and the spectrum does not evolve further with time of exposure to the dry N_2 flow. FTIR spectra were recorded between 4000 and 800 cm^{-1}. Each spectrum was obtained by averaging 256 scans recorded at a resolution of 2 cm^{-1}. Three samples from each culture were analysed by FTIR, thus generating a total of nine spectra (3×3) per condition for statistical validation, as previously described [18].

2.6. Data analysis

2.6.1. Pre-treatment of the spectra

Mass spectra were smoothed using a 5 points Savitzky–Golay algorithm. A lock mass calibration was realized for improving the mass measurement accuracy using the peaks at m/z 760.5869 and 794.5454 for positive ion and negative ion mass spectra, respectively. Mass spectra were then vector normalized between m/z 600 and 850 for positive ion mass spectra and between m/z 600 and 900 for negative ion mass spectra.

The FTIR data were preprocessed as follows. Water vapour contribution was first subtracted, and spectra were baseline-corrected and normalized for equal area between 1765 and 950 cm^{-1}. FTIR spectra were finally smoothed at a final resolution of 4 cm^{-1} by apodization of their Fourier transform by a Gaussian line [24,25].

2.6.2. Unsupervised statistical analysis

Original data yield a total of 4×10^6 and 10^7 points for each positive ion and negative ion mass spectra, respectively, which make them difficult to handle. To reduce this huge number of potential variables, positive ion mass spectra were first rescaled between m/z 700 and 850 and negative ion ones between m/z 600 and 900. Second, they were resampled from 0.0001 to 0.01 m/z. Yet the number of variables hold in each spectra, MS or FTIR, remains very large. Principal component analysis (PCA) is an unsupervised statistical method that enables reduction of the variables by building linear combinations of wavenumbers that co-vary [26]. Basically diagonalization of the covariance matrix of the data provides new variables, the so-called principal components, holding all the correlated original variables on which original spectra are finally projected. The first principal component accounts for most of the variance present in the data set; the second is built with the residual variance and is uncorrelated to the first one. The subsequent components are constructed the same way and account for the residual variance. In practice, almost all the variance of the original data can be explained with three or four first principal components, reducing the description of each spectrum to three or four numbers. Simultaneously, these weights allow an unsupervised classification of the spectra as such an observation does not suppose any a priori condition on these groups [26]. In the analyses reported here, the collection of spectra was mean-centered (the mean was removed from the individual spectra).

Table 1
Major peaks displayed in difference mass spectra recorded in positive ion mode. The lipids associated with these peaks were identified after fragmentation by collision-induced dissociation and possible assignments were displayed (headgroup and acyl chains).

Mass	Headgroup	Possible acyl chains	
		1	2
758.6	PC	16:1	18:0
768.6	PE	18:0	20:4
782.6	PC	18:0	18:1
784.6	PC	18:0	18:2
796.6	PE	18:0	22:4

Ward's linkage is another non supervised method allowing hierarchical clustering of *n* groups with minimum loss of information. It is based on the similarity of group members with respect to many variables [27]. The grouping is based on the error sum of square criterion (ESS). At each step of the grouping procedure, each possible union is considered and the two items with the lower ESS are grouped. The process is repeated until the number of groups is reduced from *n* to 1 [28].

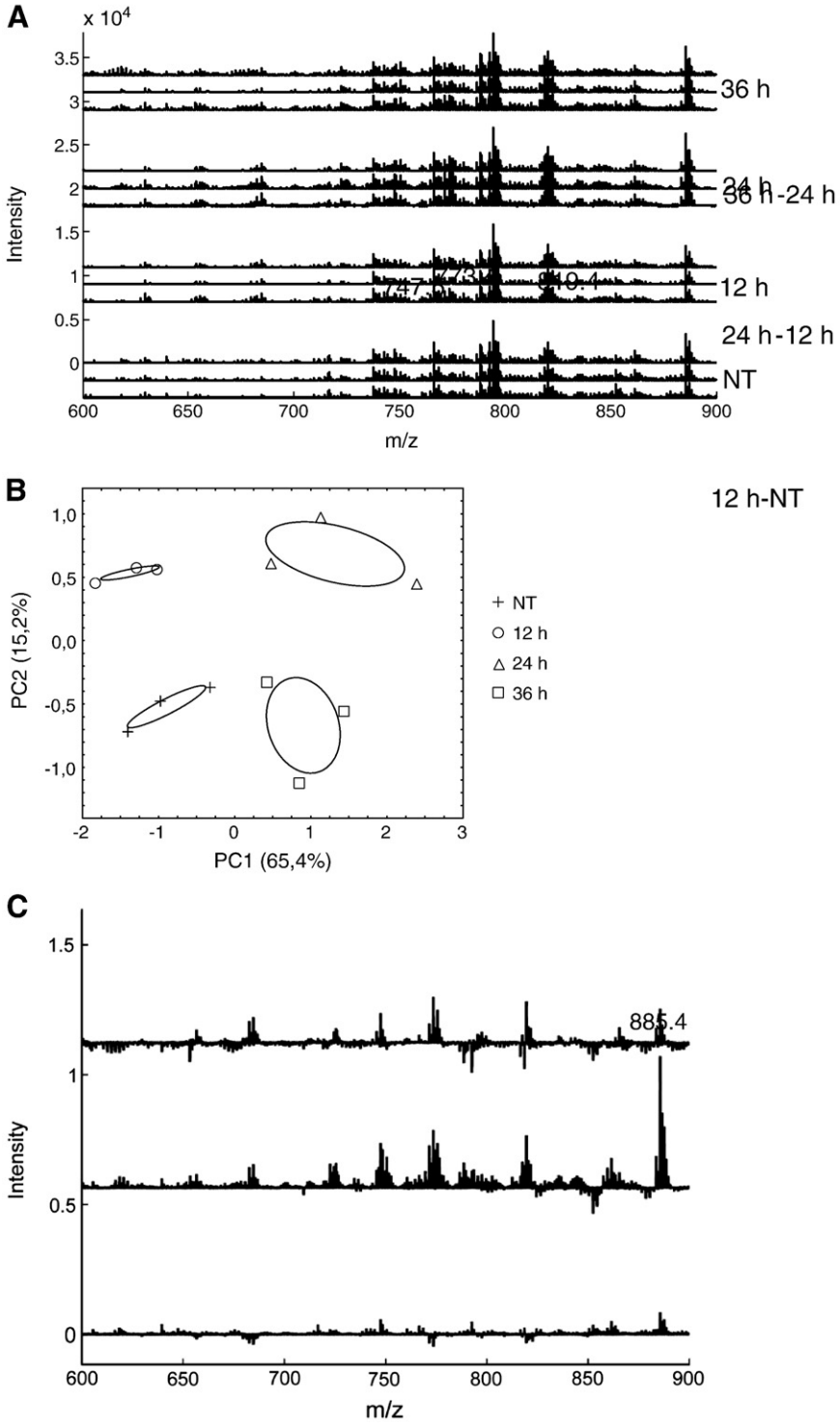

Fig. 2. (A) Mass spectra (negative ion mode) of lipid extracts from PC-3 cells incubated in the presence of ouabain for different periods of time. Every spectrum has been rescaled at the same intensity of the major peak, i.e., m/z 794.5454. Each mass spectrum originates from an independent cell culture. NT, 12, 24 and 36 are respectively lipids from cells exposed for 0, 12, 24 and 36 h to the drug. Spectra have been offset for better readability. (B) PCA performed on the mass spectra presented in A. Each symbol is the projection of one original mass spectra projected in the space of the two first principal components. *, ○, Δ, □ are lipids from cells exposed respectively to 0, 12, 24 and 36 h to 36 nM ouabain. Numbers between brackets represent the percentage of variance hold in each principal component. 95% confidence interval ellipses are presented. (C) Difference between pairs of mean mass spectra from successive conditions.

2.6.3. 2D hetero-spectral correlation analysis

In order to compare both techniques, Pearson's correlation coefficient was calculated. Pearson's correlation coefficients of a set of n observations along the variable is given by

$$r_{xy} = \frac{Cov(X,Y)}{s_x s_y}$$

where Cov(X,Y) is the covariance matrix of the data, s_x and s_y are the sample standard deviations of *X* and *Y*.

Mass spectra were processed and centered using MassLynx 4.0 (Waters, Milford, USA). Correction of FTIR spectra, vector normalization of mass spectra, PCA, hierarchical classification and heterocorrelation analysis were carried out by Kinetics, a custom made program, running under Matlab 7.1. (Matlab, Mathworks Inc). Confidence interval ellipses were computed with Statistica (Statsoft Inc.,Tulsa, USA).

3. Results

PC-3 cells were incubated with ouabain at its IC_{50}, i.e., 36 nM, for four different incubation times: 0 h for untreated cells, used as reference; 12 h to follow lipid early changes; 24 h for modifications after about one generation time; and, finally, 36 h for later changes. Cells were always counted and diluted to the same cellular concentration before lipid extraction. Importantly, it must be noted that the same samples were used to record mass spectra in both positive and negative mode and FTIR spectra.

3.1. Mass spectrometry

Fig. 1A reports mass spectra of the PC-3 cell lipid extracts recorded in positive ion mode. In the PCA analysis presented in Fig. 1B, each point represents one of the original mass spectra projected in the space built with the first two principal components. Principal component 1 essentially separates spectra as a function of incubation time (12, 24, 36 h) while principal component 2 isolates untreated cells. To point out the evolution of ouabain induced lipid changes inside PC-3 cells along the incubation time, incremental difference spectra were computed between successive pairs of conditions (Fig. 1C). Interestingly, some peaks seem to evolve continuously, e.g., m/z 758.6 and 784.6, while others only appear clearly at one time slot, e.g., m/z 782.6 and 767.6 between 24 h and 12 h, and m/z 795.6 between 36 h and 24 h. The lipids associated with major difference peaks evidenced on Fig. 1C were identified on the basis of their fragmentation patterns. Position of these peaks and assignments to lipids corresponding to these m/z ratios are reported in Table 1. They mainly derived from phosphatidylethanolamines (PE) and phosphatidylcholines (PC).

Mass spectra recorded in negative ion mode are reported in Fig. 2A and PCA analysis in Fig. 2B. Fig. 2C displays difference lipid mass spectra computed between successive pairs of incubation times in the presence of ouabain. The largest changes occurred between 12 and 24 h of ouabain incubation. Major difference peaks were fragmented and assignments to corresponding lipids are reported in Table 2. They mainly derived from phosphatidylglycerol (PG). The peak at m/z 819.5 was found to be sphingomyelin. Evolution of the same lipid can be observable at m/z 786.5 in positive ion mode. The difference in m/z value between negative and positive ion modes is assigned to the presence of chloride adduct ion, which compensates for the positive charge of the choline head. In turn, upon fragmentation a characteristic neutral loss of 50 was observed, corresponding to a methyl chloride [29]. Finally, modification of the level of one phosphatidylinositol (PI) species was also highlighted at m/z 885.5 after 24 h of ouabain exposure.

Table 2
Major peaks displayed in difference mass spectra recorded in negative ion mode. The lipids associated with these peaks were identified after fragmentation by collision-induced dissociation and possible assignments were displayed (headgroup and acyl chains).

Ion mass	Headgroup	Possible acyl chains	
		1	2
684.6	PG	18:2	16:1
747.5	PG	16:0	18:1
773.5	PG	18:1	18:1
819.5	SM	18:1	22:0
885.5	PI	18:0	20:4

3.2. FTIR spectroscopy

Mid-IR spectra of lipid samples are presented on Fig. 3A in the two spectral regions where lipid absorbances occur. PCA of the FTIR spectra is presented on Fig. 3B. It clearly shows that principal component 1 describes the evolution of lipid composition with incubation time. It account for ca. 90% of the total variance. Principal component 1 is shown on Fig. 3C. Infrared region comprised between 3025 and 2800 cm^{-1} was positively affected by ouabain treatment. It can be assigned to lipid acyl-chains ν(C-H) on unsaturated carbon (3025–3000 cm^{-1}) on one hand and ν (CH_2) or ν (CH_3) (3000 and 2800 cm^{-1}) on the other hand [12]. Region around 1740 cm^{-1}, assigned to the ester carbonyl stretching vibration, was also positively modified by the action of the drug. On the contrary, a negative contribution was observed for the phosphate stretching (around 1240 and 1085 cm^{-1}). This picture suggests an overall decrease of lipids bearing a phosphate group and/or an increase of lipid not containing phosphate, such as sphingolipid or glycerides, along the incubation time.

3.3. 2D hetero-spectral correlation analysis

While FTIR absorption bands can be assigned to specific chemical groups, for instance the phosphatidylcholines, MS peaks can be assigned to specific molecules. In order to evaluate the strength of the linear association between the variables recorded by both methods, we performed 2D correlation analysis between mass and FTIR spectra. Surprisingly, only poor correlation occurred between mass spectra and infrared bands related to $\nu_{as}(CH_2)$, $\nu_s(CH_2)$, $\nu_{as}(CH_3)$, $\nu_s(CH_3)$ (i.e., between 3025 and 2800 cm^{-1}). This indicates that the overall global changes in lipid chains could not be correlated with any particular lipid species resolved by mass spectrometry. This is consistent with the fact that all lipid contributions are overlapped in this infrared spectral range. In turn, correlations between mass spectra and 3025–2800 cm^{-1} IR spectral region were not shown.

Fig. 4 displays correlation between FTIR spectra in the 1765–950 cm^{-1} range and mass spectra acquired in negative ion mode. For the sake of clarity, only correlation coefficients comprised between 0.8 and 1, i.e., strong positive correlations, are reported as a contour map. It can be observed that only a few infrared spectral regions are strongly correlated to mass spectra. Interestingly, strong correlations were found between selected mass peaks and the infrared band around 1485 cm^{-1}, only present in choline head group of PC and sphingomyelin but not in PE, PG, PI or other lipid such as cardiolipin and cholesterol. In turn corresponding correlated MS peaks can be assigned to either PC or SM with different acyl-chain lengths or increasing number of unsaturation. The pattern is repeated several times for every m/z between m/z 735.5 and 740.5, m/z 750.5 and 753.5, m/z 762.5 and 766.5, m/z 792.5 and 793.5, m/z 816.5 and 820.5. After fragmentation, these peaks were proved to be either PC or SM and could be assigned to

different species differentiated by their insaturation levels with chain lengths from C14 to C22. It is important to underline here the use of hydrogen chloride in the lipid extraction process. In turn, PC and sphingolipids were visible on mass spectra recorded in negative ion mode, yet with and additional mass corresponding to chloride ion. In addition, some of these peaks were already

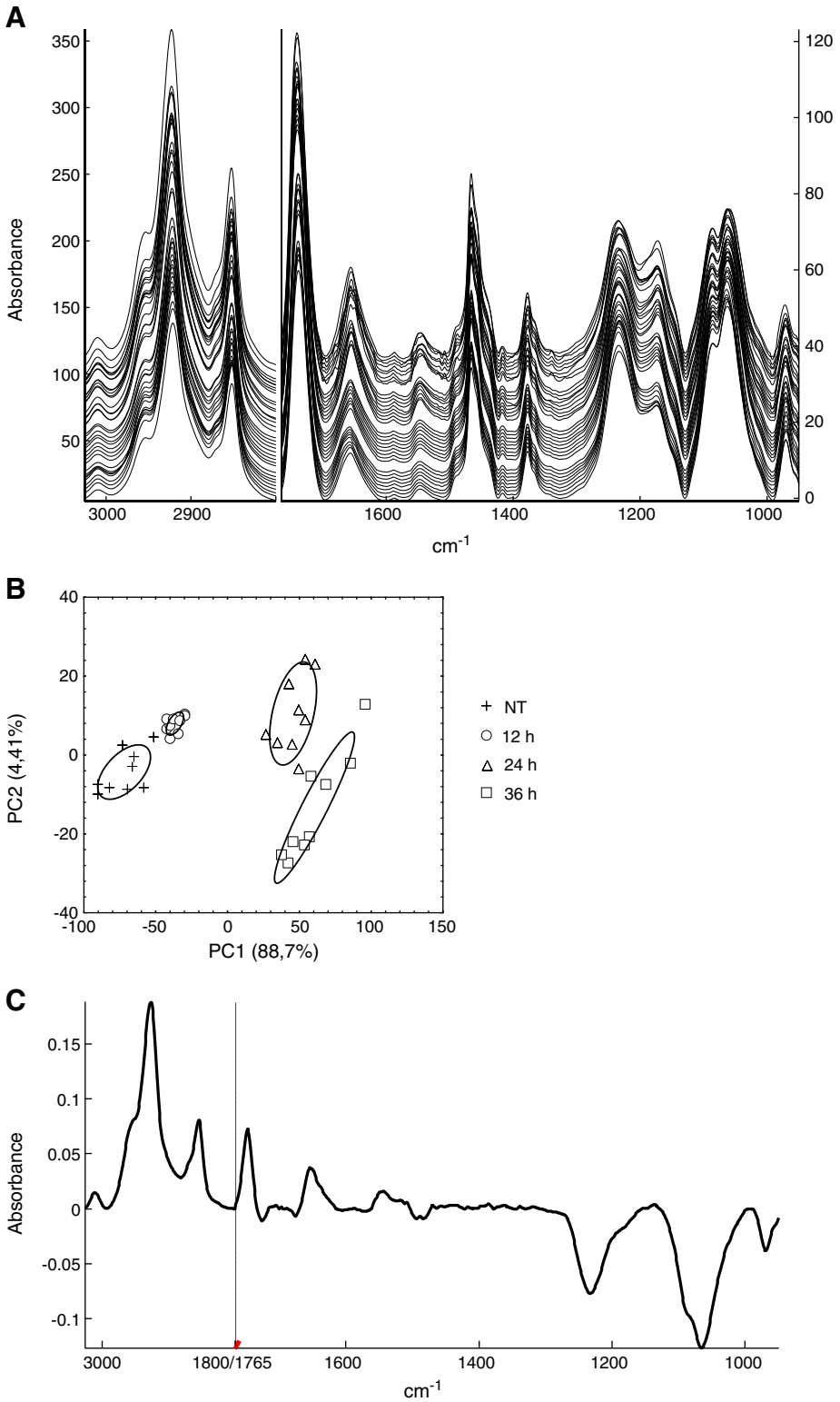

Fig. 3. (A) FTIR spectra of PC-3 lipid extracts presented between 3025–2800 cm^{-1} and 1765–950 cm^{-1}. For each culture boxes, 3 independent spectra were recorded, generating 9 spectra by condition. All spectra were rescaled for same area between 3025–950 cm^{-1} and 1765–950 cm^{-1}. Spectra have been offset for better readability. (B) PCA performed on FTIR spectra. Each symbol is the projection of one original mass spectrum in the space of the two first principal components. *, ○, Δ, □, lipids from cells exposed respectively to 0, 12, 24 and 36 h to 36 nM ouabain. Numbers between brackets represent percentage of variance hold in each principal component. 95% confidence interval ellipses are presented. (C) Representation of PC1 derived from PCA exposed in B.

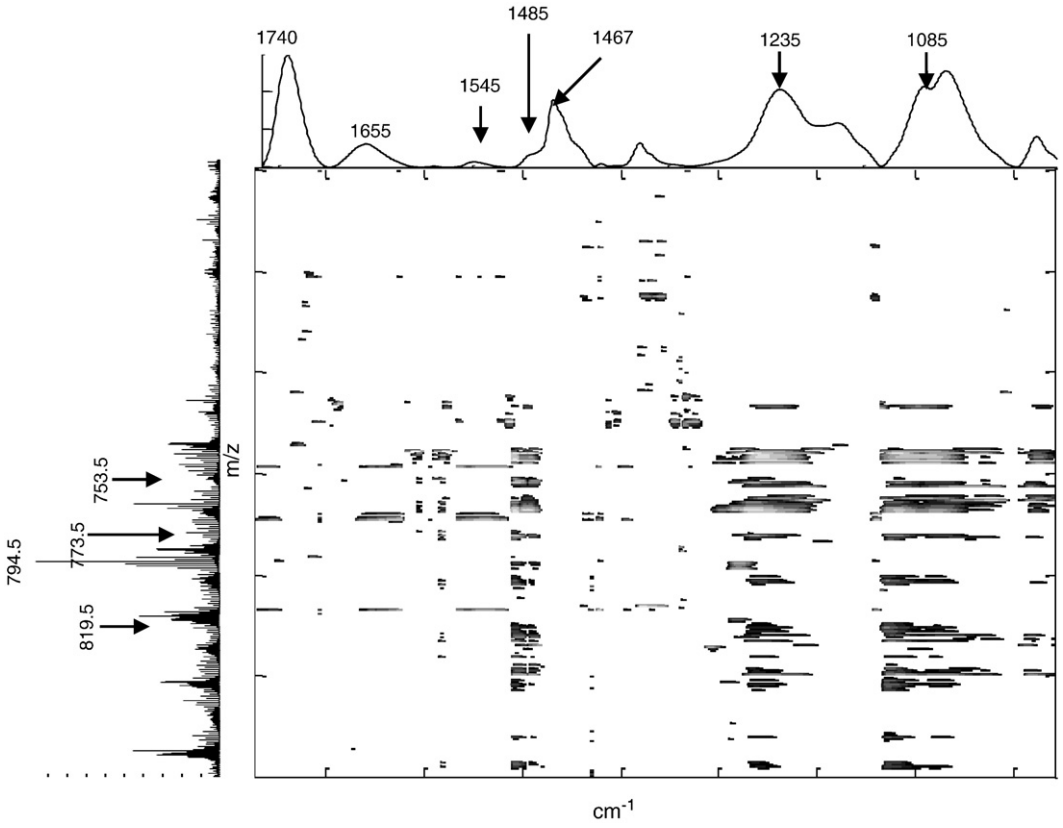

Fig. 4. Heterocorrelation between FTIR and mass spectra acquired in negative ion mode. The map represents intensity of Pearsons' correlation coefficients between intensities of each pair of m/z value and infrared absorbance. In turn, correlation coefficients are comprised between −1 and 1. For better readability contours are drawn for correlation coefficients comprised between 0.8 and 1: (1) 735.5–740.5 correspond to PC with acyl chains from C14 to C16 and SM with acyl chains from C16 to C18; (2) 750.5–753.5 = PC: C14–C18 and SM: 2×C18; (3) 762.5–766.5 = PC: C16–C18 and SM: C16–C20; (4) 792.5 = PC: C16 and C18, 793.5 = SM: C18 and C20; 5. 816.5–820.5 PC: C16–C20 and SM C18–C22.

pointed out in MS spectra recorded in positive ion mode (Fig. 1C). In particular, m/z 792.5 corresponds to 758.6 m/z in positive ion mode as well as the correlation peaks between m/z 816.5 and 820.5 which are found without Cl^- at m/z 782.5–786.5.

Interestingly correlation pattern of mass spectra recorded in negative ion mode with 1485 cm^{-1} infrared band was systematically also correlated with 1240 and 1080 cm^{-1} infrared bands, assigned respectively to symmetric ν_s (PO^{2-}) and asymmetric ν_{as} (PO^{2-}) phosphate vibrations [12]. In addition, these MS peaks were also correlated with infrared bands around 968 cm^{-1}, assigned to choline head vibrations [30].

The previous analysis indicates that correlation between FTIR and mass spectra recorded in negative ion mode occurred essentially between PC/Sphinomyelin but were not observed with PG, PE and PI. Yet, three species, i.e., m/z 746.4, 769.5–772.5 and 814.4, were correlated with FTIR spectral region around 1540 and 1640 cm^{-1} but had no correlation with the phosphates infrared bands. These three species have a pattern of correlation with the FTIR spectrum completely different from the one observed for PC or SM species. These three peaks were also correlated with 1740 cm^{-1}, a wavenumber typical of C=O stretching. Fragmentation of these peaks did not reveal any polar head group characteristic of lipid. This suggests that these peaks do not originate from phospholipid molecules.

3.4. Quantitative analysis of lipid modifications

The previous data indicate that four lipid species within PC-3 cell lipidome seemed to be particularly affected by ouabain incubation, i.e., PE, PC, PG and SM. To evaluate evolution of the concentration of each species, lipid extract IR spectra presented in Fig. 3A were fitted with pure lipid IR spectra of DPPC, DPPE, DPPG, SM. As the lipids essentially differ by their headgroup, little information could be brought by analysis of the IR acyl-chain typical region (3025–2800 cm^{-1}), carbonyl ester vibration (~1740 cm^{-1}) and phosphate group vibrations (1300–950 cm^{-1}). In turn, only the IR spectral region from 1700 to 1400 cm^{-1} was investigated. Evolution of each lipid species is reported at Table 3. Each fitting value was set to 100 for non treated cells. A significant decrease of about 10% for DPPC and 5% for DPPE was observed for an increase of 20% for sphingomyelin. To support this result, PCA was performed on concatenated positive and negative ion mode mass spectra (not shown). The major source of variance described by PC1 showed an inverse evolution of PC and sphingomyelin, in agreement with curve fitting of infrared spectra (Table 3). A

Table 3
Fit of the IR spectral area between 1700 and 1400 cm^{-1} computed on lipid extract spectra (Fig. 3A). These spectra were fitted with the spectra of pure DPPC (dipalmitoylphosphatidylcholine), DPPE (dipalmitoylphosphatidylethanolamine), DPPG (dipalmitoylphosphatidylglycerol) and SM (sphingomyelin). Every spectrum was normalized on the acyl-chain region (3025–2800 cm^{-1}). Fit values for lipid spectra from untreated cells (NT) were arbitrary set at 100 and were expressed in % of this value for the other conditions. Standard deviations are reported between brackets for each condition.

	NT	12 h	24 h	36 h
DPPC	100 (±1.5)	99.2 (±1.6)	90.8 (±1.1)	88.2 (±3.7)
DPPE	100 (±1.6)	99.1 (±1.8)	95.2 (±1)	95.5 (±3)
DPPG	100 (±1.8)	99.7 (±1)	100.7 (±1.6)	104.5 (±1.7)
SM	100 (±1.4)	100.4 (±1.3)	119.8 (±1.2)	120.2 (±1.1)

contribution from PG not demonstrated in FTIR spectra is also apparent. This discrepancy could be easily explained as DPPG has no specific features in the IR spectral region investigated. As DPPI also displays poor specific IR bands between 1700 and 1400 cm^{-1}, it was not included in the FTIR analysis. Yet, the principal component showed a significant contribution from a single PI species (see Table 2) correlated with SM and PG.

4. Discussion

Mass spectrometry and FTIR spectroscopy allowed the identification of lipids modified in PC-3 cells exposed to sub-lethal concentration of ouabain. Their evolution as a function of the incubation time was monitored. It was shown previously that PC-3 cells do not die in the conditions used for the present study but adjust their metabolism to the presence of ouabain and grow at a slower pace [31]. FTIR spectroscopy offers an overview of all chemical groups, i.e., lipid classes, present in the whole sample with an excellent signal/noise ratio (i.e., >3000). In addition, it does not require any sample labeling to standardize the data. Furthermore, features such as overall lipid chain length or unsaturation level can be observed on entire cells [19]. Label free and intact cell lipid analysis are extremely valuable features in the field of cellular biology and, in particular in the field of drug research as lipids are known to play a major role in physiological regulations. We compared here the achievements of FTIR spectroscopy with data obtained by mass spectrometry on the same samples. It appears that FTIR spectroscopy can identify content variations in some lipid classes, e.g., these containing choline head groups such as phosphatidylcholine and sphingomyelin. MS analysis could confirm this result as indicated by 2D heterocorrelation analysis. FTIR spectra were also able to report changes in ester/choline/phosphate ratios characterizing lipid changes induced by ouabain. Furthermore, quantization of major lipid classes (PC, PE, PG, SM) could be obtained by curve fitting of the spectra. One limitation of the technique is its inability to resolve lipid classes for which the polar heads do not display specific IR features such as PG and cardiolipin.

Overall the more apparent biological effects of ouabain on PC-3 cell lipids were modifications of sphingomyelin and phosphatidylinositol. Sphingomyelin is known to be essential messenger in many cellular processes [32,33] and its dysregulation contributes to the pathogenesis of several human diseases. Modification of these lipid species might be part of ouabain mechanism of action that drives to cell death in tumor cells. On the other hand, phosphatidylinositol-3 kinase (PI3K) has gained interest as one of the most important regulatory pathway in human cancer [34,35]. Recently it has been shown that PI3K inhibition leads to chemoresistance in human cancer cells by causing a delay in cell cycle [36]. In turn, compounds targeting PI3K as well as phosphoinositide-modifying enzymes are presently entering in clinical trial at a rapid pace [37,38]. Cardenolides, such as ouabain, are known to interact with $Na^{(+)}/K^{(+)}$-ATPase signalosome [39]. Relation between ouabain and activation of PI3K pathway has been recently reported for cardiac myocytes [40]. In turn, it raises the question of the role of PI as a consequence of ouabain binding to PC-3 cell $Na^{(+)}/K^{(+)}$-ATPase signalosome and as a crucial intermediate in PI3K response.

Acknowledgments

This research has been supported by a grant from Interuniversity Attraction Poles (IAP) P6/19 (Belgium) and the “Fonds National de la Recherche Scientifique” (FNRS), Belgium (FRFC 2.4533.10 and 2.4588.06). R.G. is the holder of a grant from the “IAP”, Université Libre de Bruxelles. E.G. is Director of Research with the “Fonds National de la Recherche Scientifique” (FNRS), Belgium.

References

[1] N. Leitinger, The role of phospholipid oxidation products in inflammatory and autoimmune diseases: evidence from animal models and in humans, Subcell. Biochem. 49 (2008) 325–350.
[2] R.W. Gross, X. Han, Unlocking the complexity of lipids: using lipidomics to identify disease mechanisms, biomarkers and treatment efficacy, Future Med. 1 (2006) 539–547.
[3] Y. Takuwa, Y. Okamoto, K. Yoshioka, N. Takuwa, Sphingosine-1-phosphate signaling and biological activities in the cardiovascular system, Biochim. Biophys. Acta 1781 (2008) 483–488.
[4] L. Suhaiman, G.A. De Blas, L.M. Obeid, A. Darszon, L.S. Mayorga, S.A. Belmonte, Sphingosine 1-phosphate and sphingosine kinase are involved in a novel signaling pathway leading to acrosomal exocytosis, J. Biol. Chem. (2010) 16302–16314.
[5] P. Gangoiti, L. Camacho, L. Arana, A. Ouro, M.H. Granado, L. Brizuela, J. Casas, G. Fabrias, J.L. Abad, A. Delgado, A. Gomez-Munoz, Control of metabolism and signaling of simple bioactive sphingolipids: Implications in disease, Prog. Lipid Res. (2010) 316–334.
[6] K. Takabe, R.H. Kim, J.C. Allegood, P. Mitra, S. Ramachandran, M. Nagahashi, K.B. Harikumar, N.C. Hait, S. Milstien, S. Spiegel, Estradiol induces export of sphingosine 1-phosphate from breast cancer cells via ABCC1 and ABCG2, J. Biol. Chem. 285 (2010) 10477–10486.
[7] G. Charron, J. Wilson, H.C. Hang, Chemical tools for understanding protein lipidation in eukaryotes, Curr. Opin. Chem. Biol. 13 (2009) 382–391.
[8] X. Han, R.W. Gross, Shotgun lipidomics: electrospray ionization mass spectrometric analysis and quantitation of cellular lipidomes directly from crude extracts of biological samples, Mass Spectrom. Rev. 24 (2005) 367–412.
[9] X.L. Han, R.W. Gross, Global analyses of cellular lipidomes directly from crude extracts of biological samples by ESI mass spectrometry: a bridge to lipidomics, J. Lipid Res. 44 (2003) 1071–1079.
[10] S. Milne, P. Ivanova, J. Forrester, H.A. Brown, Lipidomics: an analysis of cellular lipids by ESI-MS, Methods 39 (2006) 92–103.
[11] C. Wolf, P.J. Quinn, Lipidomics: practical aspects and applications, Prog. Lipid Res. 47 (2008) 15–36.
[12] D. Naumann, Infrared spectroscopy in microbiology, in: R.A. Meyers (Ed.), Encyclopedia of analytical chemistry, John Wiley & Sons Ltd, Chichester, West Sussex, 2000, pp. 102–131.
[13] M. Diem, M. Romeo, S. Boydston-White, M. Miljkovic, C. Matthaus, A decade of vibrational micro-spectroscopy of human cells and tissue (1994-2004), Analyst 129 (2004) 880–885.
[14] M. Harz, P. Rosch, J. Popp, Vibrational spectroscopy–a powerful tool for the rapid identification of microbial cells at the single-cell level, Cytom. A 75 (2009) 104–113.
[15] D. Naumann, D. Helm, H. Labischinski, Microbiological characterizations by FT-IR spectroscopy, Nature 351 (1991) 81–82.
[16] A. Gaigneaux, J.M. Ruysschaert, E. Goormaghtigh, Infrared spectroscopy as a tool for discrimination between sensitive and multiresistant K562 cells, Eur. J. Biochem. 269 (2002) 1968–1973.
[17] P. Lasch, W. Haensch, D. Naumann, M. Diem, Imaging of colorectal adenocarcinoma using FT-IR microspectroscopy and cluster analysis, Biochim. Biophys. Acta 1688 (2004) 176–186.
[18] A. Gaigneaux, C. Decaestecker, I. Camby, T. Mijatovic, R. Kiss, J.M. Ruysschaert, E. Goormaghtigh, The infrared spectrum of human glioma cells is related to their in vitro and in vivo behavior, Exp. Cell Res. 297 (2004) 294–301.
[19] R. Gasper, J. Dewelle, R. Kiss, T. Mijatovic, E. Goormaghtigh, IR spectroscopy as a new tool for evidencing antitumor drug signatures, Biochim. Biophys. Acta 1788 (2009) 1263–1270.
[20] T. Mijatovic, E. Van Quaquebeke, B. Delest, O. Debeir, F. Darro, R. Kiss, Cardiotonic steroids on the road to anti-cancer therapy, Biochim. Biophys. Acta 1776 (2007) 32–57.
[21] T. Mijatovic, L. Ingrassia, V. Facchini, R. Kiss, Na+/K+-ATPase alpha subunits as new targets in anticancer therapy, Expert Opin. Ther. Targets 12 (2008) 1403–1417.
[22] E.G. Bligh, W.J. Dyer, A rapid method of total lipid extraction and purification, Can. J. Biochem. Physiol. 37 (1959) 911–917.
[23] E. Goormaghtigh, V. Raussens, J.M. Ruysschaert, Attenuated total reflection infrared spectroscopy of proteins and lipids in biological membranes, Biochim. Biophys. Acta 1422 (1999) 105–185.
[24] A. Gaigneaux, J.M. Ruysschaert, E. Goormaghtigh, Cell discrimination by attenuated total reflection-Fourier transform infrared spectroscopy: The impact of preprocessing of spectra, Appl. Spectrosc. 60 (2006) 1022–1028.
[25] E. Goormaghtigh, FTIR data processing and analysis tools, in: A. Barth, P.I. Haris (Eds.), Biological and biomedical infrared spectroscopy, Advances in Biomedical Spectroscopy, vol. 2, IOS Press, Amsterdam, 2009, pp. 104–128.
[26] R.A. Johnson, D.W. Wichern, Principal Components, Applied multivariate statistical analysis, Prentice Hall, Upper Saddle River, 1998, pp. 458–513.
[27] J.H. Ward, Hierarchical grouping to optimize an objective function, J. Am. Stat. Assoc. 58 (1963) 236–244.
[28] R.A. Johnson, D.W. Wichern, Clustering, methods and ordination, in: R.A. Johnson, D.W. Wichern (Eds.), Applied multivariate statistical analysis, Prentice Hall, Upper Saddle River, 1998, pp. 726–799.
[29] M. Pulfer, R.C. Murphy, Electrospray mass spectrometry of phospholipids, Mass Spectrom. Rev. 22 (2003) 332–364.
[30] U.P. Fringeli, H.H. Günthard, Infrared membrane spectroscopy, Mol. Biol. Biochem. Biophys. 31 (1981) 270–332.
[31] R. Gasper, T. Mijatovic, A. Benard, A. Derenne, R. Kiss, E. Goormaghtigh, FTIR spectral signature of the effect of cardiotonic steroids with antitumoral properties on a prostate cancer cell line, Biochim. Biophys. Acta 1802 (2010) 1087–1094.

[32] A. Carpinteiro, C. Dumitru, M. Schenck, E. Gulbins, Ceramide-induced cell death in malignant cells, Cancer Lett. 264 (2008) 1–10.
[33] M.P. Wymann, R. Schneiter, Lipid signalling in disease, Nat. Rev. Mol. Cell Biol. 9 (2008) 162–176.
[34] B.T. Hennessy, D.L. Smith, P.T. Ram, Y. Lu, G.B. Mills, Exploiting the PI3K/AKT pathway for cancer drug discovery, Nat. Rev. Drug Discov. 4 (2005) 988–1004.
[35] P. Liu, H. Cheng, T.M. Roberts, J.J. Zhao, Targeting the phosphoinositide 3-kinase pathway in cancer, Nat. Rev. Drug Discov. 8 (2009) 627–644.
[36] G.T. McDonald, R. Sullivan, G.C. Pare, C.H. Graham, Inhibition of phosphatidylinositol 3-kinase promotes tumor cell resistance to chemotherapeutic agents via a mechanism involving delay in cell cycle progression, Exp. Cell Res. (2010) 3197–3206.
[37] T.D. Bunney, M. Katan, Phosphoinositide signalling in cancer: beyond PI3K and PTEN, Nat. Rev. Cancer 10 (2010) 342–352.
[38] K.K. Wong, J.A. Engelman, L.C. Cantley, Targeting the PI3K signaling pathway in cancer, Curr. Opin. Genet. Dev. 20 (2010) 87–90.
[39] Z. Xie, T. Cai, Na+-K+–ATPase-mediated signal transduction: from protein interaction to cellular function, Mol. Interv. 3 (2003) 157–168.
[40] L. Liu, X. Zhao, S.V. Pierre, A. Askari, Association of PI3K-Akt signaling pathway with digitalis-induced hypertrophy of cardiac myocytes, Am. J. Physiol. Cell Physiol. 293 (2007) C1489–C1497.